Brittle-Ductile Transition in Rocks

JAMES D. BYERLEE

U. S. Geological Survey, Silver Spring, Maryland 20910

The deformational characteristics of two limestones, one gabbro, and one dunite have been investigated as a function of confining pressure. It was found that friction of these rocks and friction of granite and serpentinite studied elsewhere are nearly identical and that the brittle-ductile transition pressure is simply the pressure at which the stress required to form a fault is equal to the stress required to cause sliding on the fault. The transition pressure is higher in extension than it is in compression. This difference occurs because the frictional shear stress required to cause sliding is determined not by confining pressure but by the principal stresses and the angle of the fault. For the same frictional shear stress on a fault surface, the confining pressure is much higher in extension than it is in compression.

INTRODUCTION

von Kármán [1911], *Robertson* [1955], *Handin and Hager* [1957], *Paterson* [1958], *Heard* [1960], *Mogi* [1966], and others found that at low confining pressure many rocks are brittle. That is, when the differential stress is sufficiently high, a fault is formed, and after faulting the compressive strength is decreased. At high confining pressure, however, the same rocks may be ductile. That is, they may fault or otherwise deform without loss of compressive strength.

A possible physical explanation for the phenomenon was given by *Orowan* [1960]. He suggested that, at high confining pressure, friction may increase to such an extent that it requires as much stress to overcome friction as it does to cause faulting; hence, strength does not drop after faulting. *Maurer* [1965] studied the friction of rocks and found that, with the exception of shale, friction does not vary significantly with rock type. Following Orowan, he suggested that the brittle-ductile transition may occur when friction along the fracture surface exceeds the shear strength of the rock. Unfortunately his experiments were not performed at sufficiently high confining pressure to test this hypothesis critically.

Mogi [1966] examined most of the published data on the fracture and yield strength of rocks and concluded that at least for the silicate rocks the frictional hypothesis was valid but for the weaker carbonate rocks the brittle-ductile transition pressure was not determined by friction. The basic assumption made by Mogi was that the coefficient of friction of rocks is independent of confining pressure. The coefficient of friction is found by dividing the shear stress required to cause sliding by the normal stress across the surfaces. *Maurer* [1965], *Handin and Stearns* [1964], *Raleigh and Paterson* [1965], and *Byerlee* [1967*a*] have shown that for rocks the coefficient of friction depends on confining pressure or normal stress, and hence Mogi's basic assumption is incorrect.

Byerlee [1967*a*] studied the frictional characteristics of granite and found that at 10 kb confining pressure the rock deforms without loss of compressive strength, because at this pressure the strength of the rock at faulting is equal to the strength after faulting.

The frictional hypothesis for the brittle-ductile transition is attractive, but previously sufficient data on the friction of rocks were not available to test the generality of this theory. This lack of frictional data is unusual considering the vast amount of research that has been done on the mechanical behavior of rocks. Friction can be determined very simply by continuing deformation after faulting. If the angle of the fault and the stresses required to cause movement are known, friction can be determined by a simple calculation. Unfortunately, in only a few cases do the data exist in the published literature. There are two reasons for the absence of these data. The first is that many investigators use copper as the jacketing material, and, when faulting occurs, the jacket is broken. The broken jacket allows the confining pressure medium to enter the rock so

TABLE 1. Description of Materials
Both limestones may contain dolomite or other impurities.

Rock	Density	Porosity	Av. Grain Diameter, mm	Modal Analysis*
Solenhofen limestone	2.663	0.048	0.01	99 Ca?
Oak Hall limestone	2.748	0.003	0.1	99 Ca?
Nahant gabbro	3.084	0.001	5.2	40 Py, 20 S, 15 Ol, 10 An_{70}, 10 Mi, 3 O
Spruce Pine dunite	3.262	0.002	0.5	96 Ol, 3 S, 1 O

* Ca, calcite; S, serpentine; O, oxides, Py, pyroxene; Ol, olivine; An, anorthite; Mi, mica.

that the effective confining pressure on the sample becomes zero. The other reason is that most investigations have been made to determine the stress at faulting, and, when faulting occurs, the experiments are terminated.

The present investigation determines friction for a number of rocks to determine whether, as in granite, the brittle-ductile transition pressure is simply the pressure at which the stress required to form a fault is equal to the stress required to cause sliding on the fault.

Experimental Method

Differential stress was measured as a function of strain for four rocks at room temperature and at confining pressures up to about 5 kb. Porosity, grain size, and modal analysis of the rocks studied are given in Table 1. Precisely ground cylinders of the rocks, 3.8 cm long and 1.58 cm in diameter, were jacketed in a gum rubber tube with a wall thickness of 3.17 mm. The ends were sealed with a wire clamped to hardened steel end plugs. It was found that after deformation the specimens fell to pieces on removal of the rubber jacket. To prevent this, a copper cylinder with a wall thickness of 0.13 mm was placed over the specimen before finally jacketing in rubber. This copper cylinder gave the specimen a slight mechanical strength, so that the rock stayed intact and permitted accurate measurement of the angle of the fault surface after completion of an experiment.

The pressure vessel used in the experiments was described by *Brace* [1964]. Axial force was applied to the piston with a ball screw driven by an electric motor through a reduction gear box. The force was measured with a load cell outside the pressure vessel. Strain rate of 2.4 × 10^{-4}/sec was maintained constant throughout the experiments. Axial displacement of the piston was measured with a Sanborn DCDT 500 transducer attached to the piston. The confining pressure was measured with a manganin coil situated inside the pressure vessel. To keep the pressure constant as the piston advanced into the pressure vessel, the volume of the hydraulic system was kept constant. This was done by automatic switching of an electric motor that advanced or withdrew a piston from an auxiliary pressure vessel connected hydraulically to the main pressure vessel. The direction of the motor was controlled by a logic discriminator circuit, which

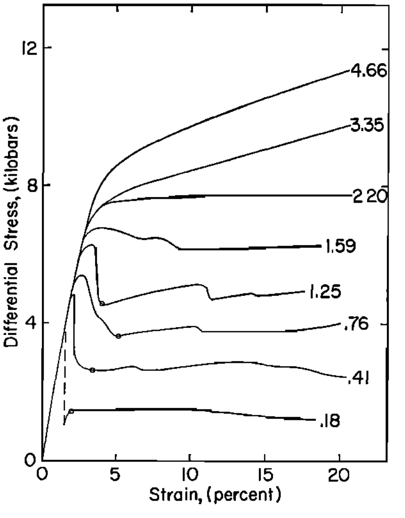

Fig. 1. Stress-strain curves for Oak Hall limestone. Uncorrected for change in length or cross-sectional area. Numbers at the ends of the curves are the confining pressures.

determined automatically whether the pressure had to be increased or decreased. The pressure could be maintained constant within ±5 bars with this device.

The output from the differential transformer measuring displacement was fed directly into one axis of a Mosely model 136 XYY recorder. The manganin coil and force cell were connected to bridge circuits, the output from which was fed into the other two axis of the recorder.

The axial force F measured by the load cell is given by

$$F = PA_p + f + \Delta\sigma A_r$$

where P is the confining pressure, A_p and A_r are the area of the piston and the rock, respectively, $\Delta\sigma$ is the differential stress in the specimen, and f is the frictional force at the O ring through which the piston moves. Before the piston comes into contact with the specimen, the force measured by the load cell is the sum of the first two terms. If the confining pressure and velocity of the piston is maintained constant throughout the experiment, these two terms remain constant. The differential stress times the cross-sectional area of the specimen was found simply by subtracting the force required to advance the piston against the confining pressure medium from the total force recorded.

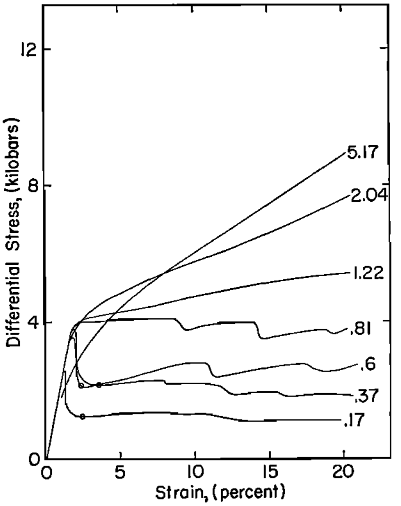

Fig. 2. Stress-strain curves for Solenhofen limestone. Uncorrected for change in length or cross-sectional area. Numbers at the ends of the curves are the confining pressures.

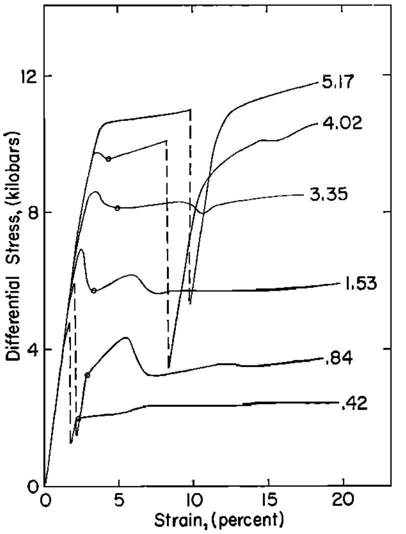

Fig. 3. Stress-strain curves for Nahant gabbro. Uncorrected for change in length or cross-sectional area. Numbers at the ends of the curves are the confining pressures.

The differential force could be measured with an accuracy of ±1%, and the axial displacement had an accuracy of better than 0.1 mm. Fault angles could not be measured with an accuracy of better than ±2° because of the irregularity of the faults, particularly the faults formed at low confining pressure.

Experimental Results

Figures 1 through 4 are typical tracings of the differential force axial displacement curves as displayed on the recorder. For clarity in the figures, some of the experimental results have not been shown. Differential stress and strain were calculated by using the initial cross-sectional area and length of the specimen. For large strains, the true stress in the specimen is different from the value shown because the area of the specimen supporting the load changes during deformation. The dashed lines in the figures indicate where deformation occurred with a sudden release of elastic energy. In all other cases the deformation occurred stably.

The differential stress at fracture, or at 5% strain if the specimen was ductile, is plotted in Figure 5 for all the experiments. The significance of the solid line in Figure 5 will be explained below. There is a change in the cross-

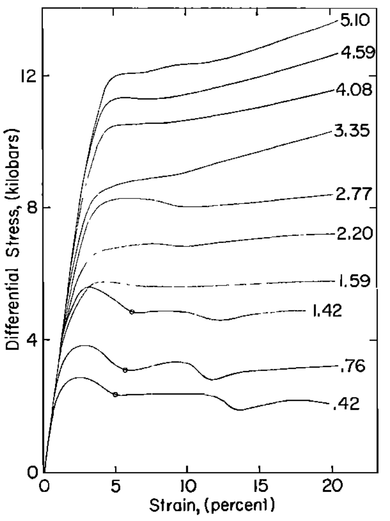

Fig. 4. Stress-strain curves for Spruce Pine dunite. Uncorrected for change in length or cross-sectional area. Numbers at the end of the curves are the confining pressures.

sectional area of the specimen, particularly in the brittle region [*Brace et al.*, 1966], but its precise value is difficult to determine. The change in area preceding fracture is small, however, and the error introduced by neglecting it does not exceed 3%.

After faulting the differential stress required to cause frictional sliding on the fault increases with displacement. The normal and shear stresses σ_n and τ across the surfaces at the minimum, indicated by open circles in Figures 1 through 4, were calculated by the equations

$$\tau = (\Delta\sigma/2) \sin 2\alpha$$

$$\sigma_n = \left(\frac{\Delta\sigma + 2p}{2}\right) - \left(\frac{\Delta\sigma}{2}\right) \cos 2\alpha$$

where α is the angle that the fault surface makes with the axis of the specimen, $\Delta\sigma$ is the differential stress, and p is the confining pressure. There is a change in the cross-sectional area of the specimen supporting the load as movement occurs on the fault surface. This area change was corrected for use is calculating the stresses. The results from all the experiments are plotted in Figure 6.

Near the pressure of the brittle-ductile transition, multiple faulting occurs and there is considerable uncertainty in the cross-sectional area of the specimen at any point on the stress-strain curve. For this reason, the data near the transition could not be used to calculate friction. More than one fault was also formed at lower pressures, but the distance of sliding between successive faults was large. The initial fault could be easily identified, and there was no ambiguity in identifying the minimum on the stress-strain curves. The number of faults formed in the specimen was equal to the number of downward breaks in the stress-strain curves. It was assumed that these discontinuities indicated faulting. This assumption was checked in the following way. When two conjugate faults were formed, displacement on the second fault was calculated from the angle of the fault and the axial displacement. This distance was found to be equal to the offset of the first fault. The angle that the faults made with the axis of the specimen increased with an increase in confining pressure, and near the brittle-ductile transition pressure it was about 30°.

Discussion

Stress-strain curves for Cabramurra serpentinite, in which deformation was continued after faulting, have been published by *Raleigh and Paterson* [1965]. The frictional shear stress and normal stress were calculated from their stress-strain curves and an average fault angle of 30°. The results are plotted in Figure 6. Frictional data for sliding on mated surfaces of granite [*Byerlee*, 1967*a*, *b*] are also shown.

It should be noted that, on surfaces of granite, the differential stress required to cause sliding decreases slightly with displacement, whereas, on surfaces of the rocks in this study, it increased with displacement. Also, in the case of granite, sliding occurs by stick slip; that is, movement is accompanied by a sudden release of elastic energy, whereas movement between the surfaces of the rock studied here generally took place smoothly. A necessary condition for stick slip to occur is that the frictional stress must decrease with displacement [*Rabinowicz*, 1965], and this seems to be borne out here. This study shows that some rocks deform by stick slip and others do not, and this may have important consequences if sudden movement on a pre-existing fault is responsible for crustal earthquakes [*Brace and Byerlee*, 1966]. The phenomenon of stick slip has been studied in detail, and the results will be presented in a later paper.

Figure 6 shows that at low pressures the frictional shear stress increases rapidly as normal stress increases. Beyond 2 kb, the frictional stress rises less rapidly and there is a nearly linear relationship between shear and normal stress. *Byerlee* [1967*a*, *b*] studied the friction of granite in detail and gave the following explanation for the relationship between shear and normal stress for sliding. At low normal stresses, surfaces may slide by lifting over the irregularities on the surfaces. The shear stress required to do this is determined by the angle made by the irregularities with the plane of sliding. A larger shear stress is required to lift the surfaces over one another if the asperities are steep than is required if they are inclined at a lower angle. For a fixed configuration of the surfaces in contact, the shear stress required to cause sliding in this manner increases linearly as normal stress increases. A stage is reached, however, at which it is easier to slide by breaking through the asperities than by lifting over them. In the case of granite, this point seems to occur at a normal stress of about 2 kb, and, beyond this point, the increase in frictional shear stress with normal stress represents the change in strength of the material with pressure. At normal stresses between about 100 bars and 2 kb, the behavior is transitional. That is, the most steeply inclined asperities break, but the surfaces may lift over the less steeply inclined ones. In this region there is

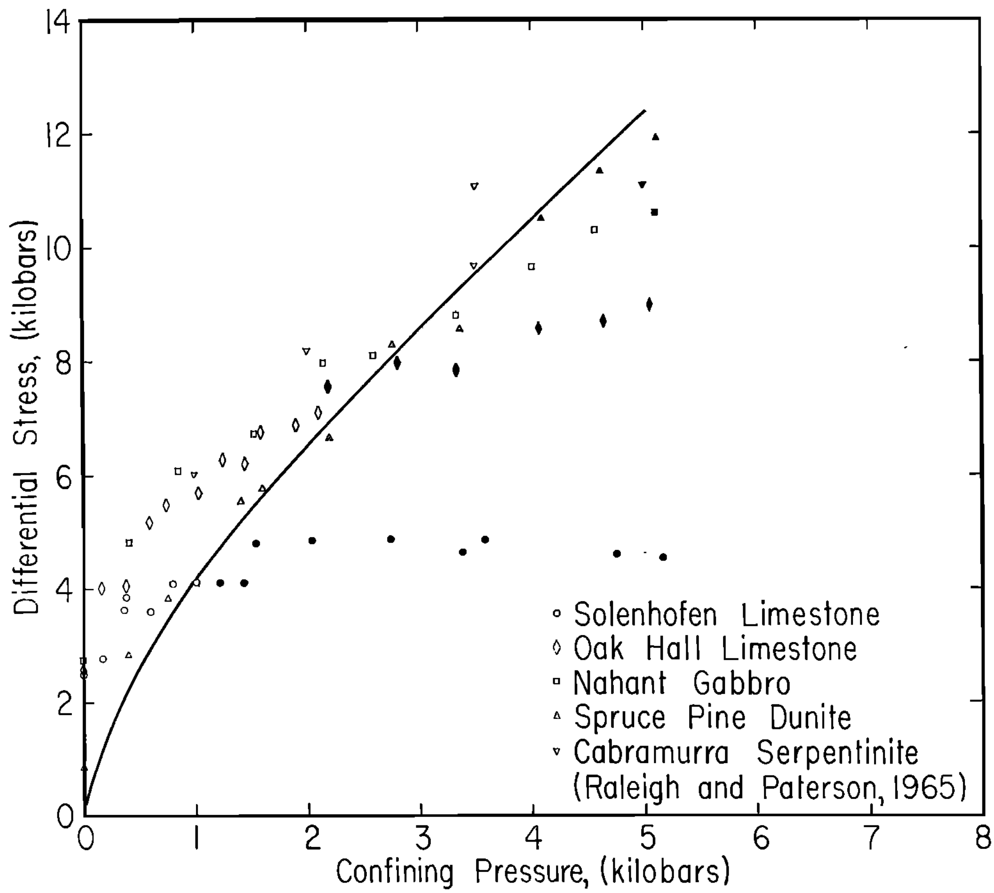

Fig. 5. Differential stress versus confining pressure at fracture or 5% strain if the specimen was ductile. Open symbols indicate brittle behavior; closed symbols, ductile. Solid line is the boundary between the brittle and ductile regions determined from friction data (Figure 6).

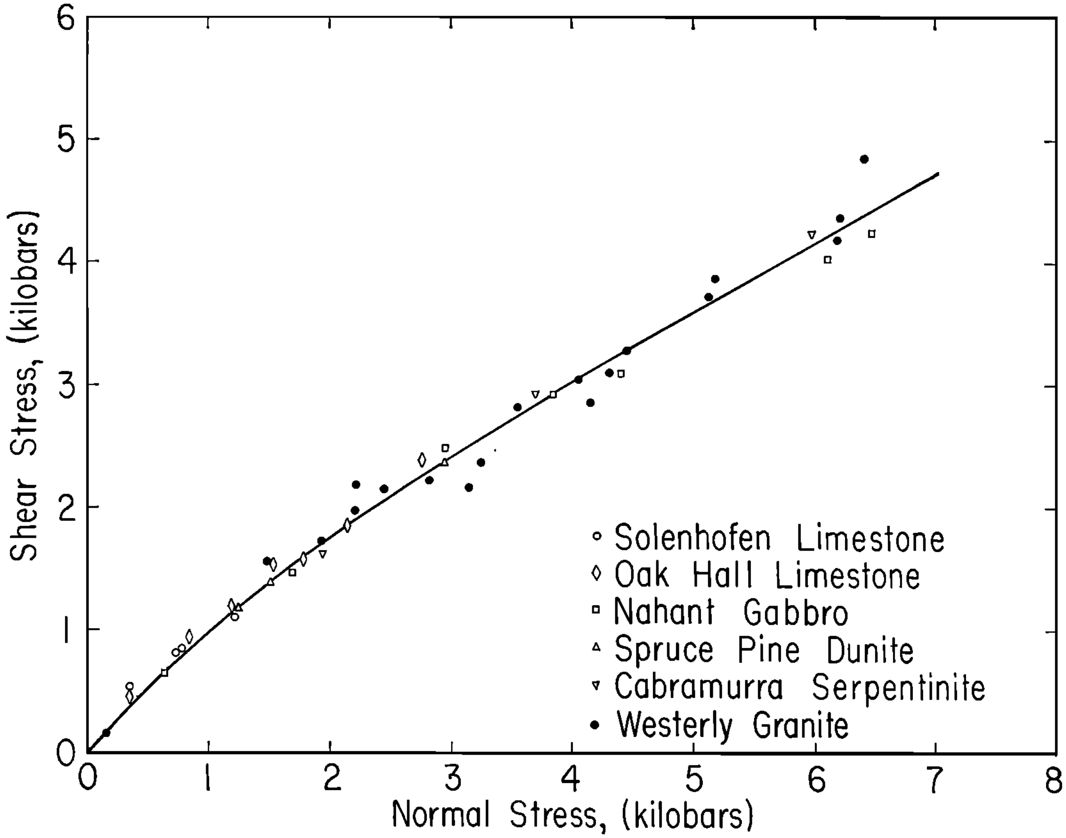

Fig. 6. Shear stress versus normal stress for friction. Cabramurra serpentinite data from *Raleigh and Paterson* [1965] and Westerly granite data from *Byerlee* [1967*a*, *b*].

a nonlinear increase of the frictional shear stress with normal stress.

This explanation is consistent with the results presented here for other rock types.

The most remarkable feature of the friction of rocks as shown in Figure 6, is that it is almost independent of rock type. *Maurer* [1965] also found this to be true at low normal stresses. *Byerlee* [1967*b*] developed a theory of friction based on brittle fracture. The theory predicts that, when contact is made only at the tips of asperities, the coefficient of friction, which is the ratio of shear to normal stress, should be independent of the material and have a value of 0.1. For geometrical situations that were close to the theoretical model this prediction was found to be correct. The theory could not, however, be extended to a general situation in which the irregularities on the surfaces were completely interlocked. From the present results, however, where there is almost certainly a high degree of interlocking, it seems that friction is almost independent of the material.

It was found in the present study that, near the pressure of the brittle-ductile transition, the angle that the fault surfaces made with the axis of the specimens was close to 30° for all the rocks. The reason for this is not clear, but it seems to be generally true for rocks [*Handin and Hager,* 1957]. Perhaps this phenomenon is related in some way to the fact that friction is nearly independent of mineralogy for interlocked surfaces.

Before we discuss the brittle-ductile transition, we will first transform the line through the points in Figure 6 into $\Delta\sigma$, p coordinates by means of the equations

$$\tau = (\Delta\sigma/2) \sin 2\alpha$$

$$\sigma_n = \left(\frac{\Delta\sigma + 2p}{2}\right) - \left(\frac{\Delta\sigma}{2}\right) \cos 2\alpha$$

If the angle α, which the fault surface makes with the axis of the specimen, is 30°, the above equations reduce to

$$\Delta\sigma = 2.31\tau$$

$$p = \sigma_n - 0.58\tau$$

The transformation was carried out numerically, and the result is shown as a solid line in Figure 5.

If the friction hypothesis for the brittle-ductile transition in rocks is valid, the rock will be brittle if at any confining pressure the differential stress that a rock can support at failure falls above the line; the rock will be ductile if the differential stress falls below the line. In other words, the brittle-ductile transition pressure should be the pressure at which the stress required to form a fault is equal to the stress required to cause sliding on the fault. Figure 5 shows that this statement seems to be true for the rocks studied here. The open symbols to the left of the line represent brittle behavior; the solid symbols to the right of the line represent ductile behavior. Slight departures can be accounted for by the small dependence of friction on rock type. For example, the transition pressure is slightly lower for Oak Hall limestone and slightly higher for Nahant gabbro than the values predicted. From Figure 6, however, it can be seen that the frictional shear stress of Oak Hall limestone is slightly higher and that of Nahant gabbro, which is slightly lower than the line used in calculating the boundary between the brittle and ductile regions.

Mogi [1966] has collected from the published literature the strength data for a wide variety of rock types. These data are shown in Figure 7 for the silicate rocks and in Figure 8 for the weaker carbonate rocks. The open circles represent brittle behavior and the closed circles ductile behavior. Mogi labeled the ordinate in his figures axial strength. The original data were checked, and it was found that axial strength is, in the notation used in this paper, differential stress. Mogi divided the brittle and the ductile regions by a straight line, shown as the dashed lines in Figures 7 and 8. The transition pressure in silicate rocks fell near this line, but, for the weaker carbonate rocks, the transition took place at much lower pressures. He inferred from this that the friction hypothesis for the brittle-ductile transition may be correct for the silicates but friction could not be the controlling mechanism for the carbonates. The basic assumption made by Mogi was that the coefficient of friction for rocks is independent of confining pressure. The boundary between the two regions should therefore be a straight line passing through the origin.

The present work shows that his basic assumption was incorrect. The solid line in Figures 7 and 8 is the friction boundary line between the two regions found in this study, and

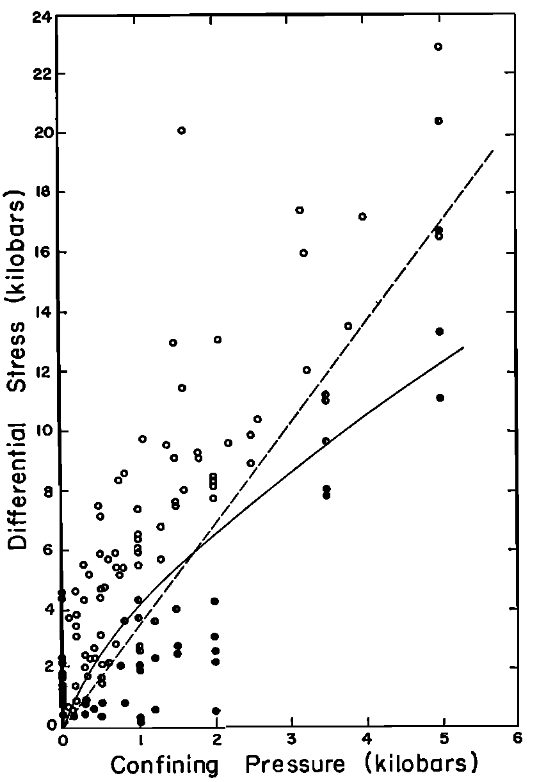

Fig. 7. Differential stress versus confining pressure for silicate rocks [from *Mogi*, 1966]. Solid line is the boundary between the brittle and ductile regions determined from friction data. Dashed line is the friction boundary suggested by Mogi. Open symbols indicate brittle behavior; half closed symbols, transitional; closed symbols, ductile.

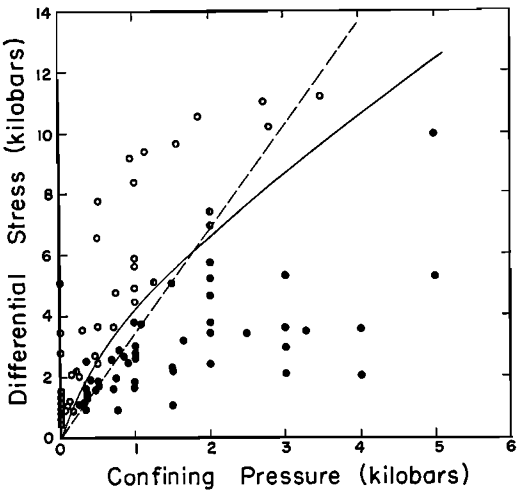

Fig. 8. Differential stress versus confining pressure for carbonate rocks [from *Mogi*, 1966]. Solid line is the boundary between the brittle and ductile regions determined from friction data. Dashed line is the friction boundary suggested by Mogi. Open symbols indicate brittle behavior; half closed symbols, transitional; closed symbols, ductile.

the transition pressure for both the silicates and the carbonates falls close to this line. The frictional hypothesis seems, therefore, to be generally true for most rock types. *Mogi* [1966] found that the transition pressure for shale is very much higher, but this higher pressure seems to occur because the frictional shear stress required to cause sliding on surfaces of shale at any given normal stress is very much lower than it is for other rocks [*Maurer,* 1965]. For the weaker silicates in Figure 7, the transition pressure seems to be slightly higher than the value predicted. The transition pressure is also slightly higher for porous tuffs; it would be of interest to find out whether this relation occurs because this rock type has lower friction than other rocks.

Heard [1960] has found that the brittle-ductile transition pressure is very much higher in extension than it is in compression. Before it can be determined whether the friction hypothesis is valid for extension, friction must first be converted into this new coordinate system. In extension

$$\tau = (\Delta\sigma/2)\sin 2\alpha$$

$$\sigma_n = \left(\frac{2p - \Delta\sigma}{2}\right) - \left(\frac{\Delta\sigma}{2}\right)\cos 2\alpha$$

where α is the angle that the fault surface makes with the maximum principal stress. In extension, *Heard* [1960] found that for Solenhofen limestone near the transition pressure the angle is about 20°. With this value the above equations reduce to

$$\Delta\sigma = 3.11\tau$$

$$p = \sigma_n + 2.75\tau$$

The transformation was made numerically, and the result is plotted as a solid line in Figure 9.

This line should mark the boundary between brittle and ductile behavior in extension. The open symbols in the figure represent brittle behavior; the solid symbols, ductile behavior. The circles were plotted from the data published by *Heard* [1960]; the triangles, from the data published by *Handin et al.* [1967]. The brittle-ductile transition takes place at a pressure slightly below the predicted value, but, considering the uncertainties in the strength, friction, and fault angle, the transition pressure in extension is consistent with the friction hypothesis.

It may well be argued that the intermediate stress may have an effect on friction, but *Byerlee* (1967*a* and more recent unpublished results) has shown that, for granite in compression, the frictional shear stress at any given normal stress is the same for sliding surfaces inclined at 30° and 45° to the axis of the specimen. For example, at a normal stress of 8 kb, the shear stress required to cause sliding on surfaces of granite is 5.3 kb for both 30° and 45°. In both cases the intermediate stress is the confining pressure *P*. If the angle is 45°, *P* is 2.7 kb, but it is 4.94 kb if the angle is 30°. This indicates that within the experimental error, the intermediate stress has no effect on friction.

One question that still remains unanswered is what determines the stress a rock will support at any given confining pressure. There is at present no satisfactory theory to predict the stress required to form a fault surface in rocks in the brittle region [*Brace and Byerlee,* 1967]. In the ductile region, it is also not clear just what determines the stress that a rock will support. In some rocks, particularly limestones, plastic deformation of the individual crystals may occur during deformation; for fully plastic materials, the yield stress-and-strain hardening

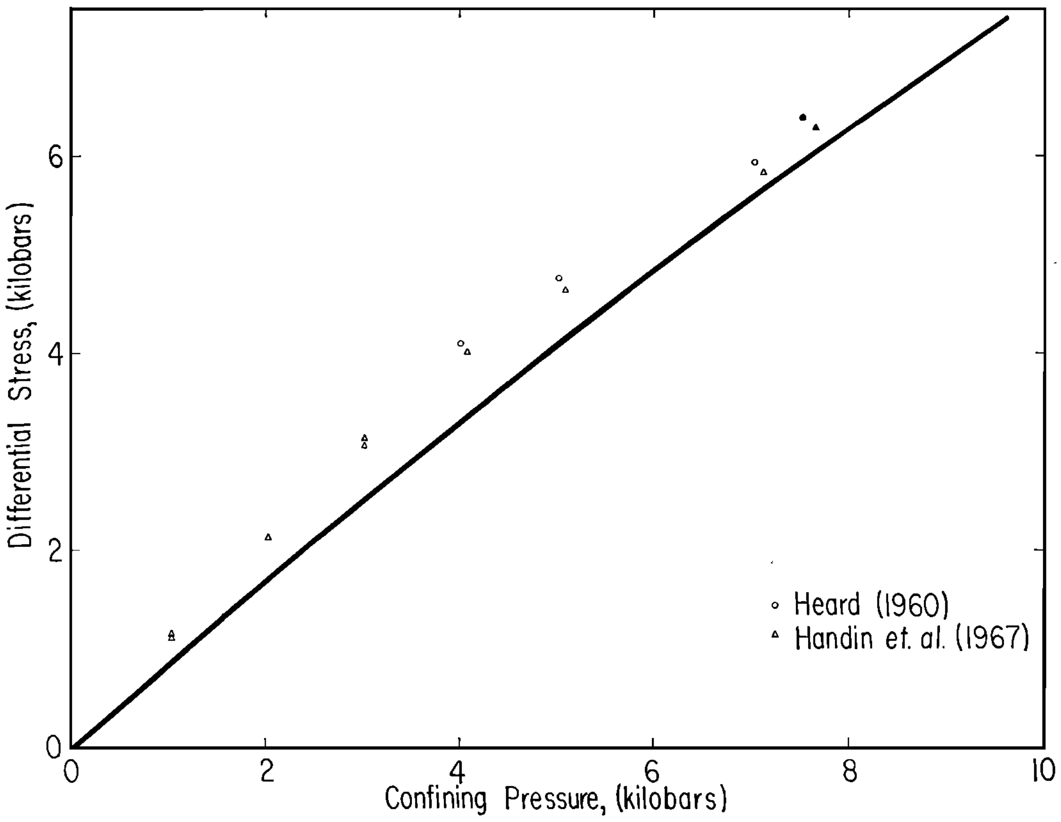

Fig. 9. Differential stress versus confining pressure at fracture or 5% strain for Solenhofen limestone in extension. Solid line is the boundary between the brittle and ductile regions determined from friction data. Open symbols indicate brittle behavior; closed symbols, ductile.

rate is almost independent of confining pressure. These effects are illustrated by the work of *Paterson* [1964]. He showed that, for copper, the stress-strain curve at a pressure of 8 kb does not differ by more than a few per cent from the curve at atmospheric pressure. This is clearly not true for limestone. Figures 1 and 2 show that the strain strengthening rate increases remarkably with confining pressure.

Cataclasis (that is crushing of the grains) may be the controlling mechanism of deformation at room temperature over the confining pressure range investigated. At present, however, there is no theory that can be used to predict either the stress required to deform a rock in this manner or the effect confining pressure should have on the strain strengthening rate. Clearly the problem requires further work.

The present experiments were performed at room temperature and at strain rates of 2.4×10^{-4}/sec. Recent unpublished results for granite show that, within the experimental error, friction is not different at strain rates of 2.4×10^{-6}/sec and 2.4×10^{-4}/sec. The effect of strain rate on the friction of other rock types remains to be determined, however, high temperature and chemical environment may also have an effect on friction, and this possibility should be investigated.

The present work shows that the brittle-ductile transition pressure in rocks at room temperature both in compression and in extension is the pressure at which the stress required to form a fault surface is equal to the stress required to cause sliding on the fault.

Acknowledgments. The research facilities at the Massachusetts Institute of Technology were made available through the courtesy of Professor W. F.

Brace. Professor Brace, Drs. L. Peselnick, C. B. Raleigh, and E. C. Robertson read the manuscript and suggested a number of improvements.

The investigation, which was carried out at the Department of Geology and Geophysics, Massachusetts Institute of Technology, was supported by Air Force Cambridge Research Laboratories, Office of Aerospace Research, U. S. Air Force, Bedford, Massachusetts, under contract AF 19(628)-3298. Publication authorized by the Director, U. S. Geological Survey.

References

Brace, W. F., Brittle fracture of rocks, in *State of Stress in the Earth's Crust,* edited by W. R. Judd, pp. 110–178, American Elsevier, New York, 1964.

Brace, W. F., and J. D. Byerlee, Stick slip as a mechanism for earthquakes, *Science, 153*(3739), 990–992, 1966.

Brace, W. F., and J. D. Byerlee, Recent experimental studies of brittle fracture of rocks, in *Failure and Breakage of Rock,* edited by C. Fairhurst, pp. 58–81, American Institute of Mining, Metallurgical, and Petroleum Engineers, New York, 1967.

Brace, W. F., B. W. Paulding, Jr., and C. Scholz, Dilatancy in the fracture of crystalline rocks, *J. Geophys. Res., 71*(16), 3939–3953, 1966.

Byerlee, J. D., Frictional characteristics of granite under high confining pressure, *J. Geophys. Res., 72*(14), 3639–3648, 1967*a*.

Byerlee, J. D., Theory of friction based on brittle fracture, *J. Appl. Phys., 38*(7), 2928–2934, 1967*b*.

Handin, J., and R. V. Hager, Experimental deformation of sedimentary rocks under confining pressure: Tests at room temperature on dry samples, *Bull. Am. Assoc. Petrol. Geologists, 41,* 1–50, 1957.

Handin, J., H. C. Heard, and J. M. Magouirk, Effect of the intermediate principal stress on the failure of limestone, dolomite, and glass at different temperatures and strain rates, *J. Geophys. Res., 72*(2), 611–640, 1967.

Handin, J., and D. W. Stearns, Sliding friction of rock (abstract) *Trans. Am. Geophys. Union, 45*(1), 103, 1964.

Heard, H. C., Transition from brittle fracture to ductile flow in Solenhofen limestone as a function of temperature, confining pressure, and interstitial fluid pressure, *Rock Deformation, Geol. Soc. Am. Mem., 79,* 193–226, 1960.

Maurer, W. C., Shear failure of rock under compression, *Soc. Petrol. Engrs. J., 5,* 167–175, 1965.

Mogi, K., Pressure dependence of rock strength and transition from brittle ductile flow, *Bull. Earthquake Res. Inst. Tokyo Univ., 44,* 215–232, 1966.

Orowan, E., Mechanism of seismic faulting, *Rock Deformation, Geol. Soc. Am. Mem., 79,* 323–345, 1960.

Paterson, M. S., Experimental deformation and faulting in Wombeyan marble, *Bull. Geol. Soc. Am., 69,* 465–476, 1958.

Paterson, M. S., Triaxial testing of materials at pressures up to 10,000 kg/cm² (150,000 lb./sq. in.), *J. Inst. Engrs., Australia,* 23–30, Jan.–Feb., 1964.

Rabinowicz, E., *Friction and Wear of Materials,* John Wiley, New York, 1965.

Raleigh, C. B., and M. S. Paterson, Experimental deformation of serpentinite and its tectonic implications, *J. Geophys. Res. 70*(16), 3965–3985, 1965.

Robertson, E. C., Experimental study of the strength of rocks, *Bull. Geol. Soc. Am., 66,* 1275–1314, 1955.

von Kármán, Th., Festigkeits Versuche unter all suitigem Druck, *Verhandl. deut. Ingr., 55,* 1749–1757, 1911.

(Received December 29, 1967.)